Inkjet-printed Dry Flexible Electromyography Electrode Array for Classifying Finger Movements with AI Algorithms

Nabonita Mitra, Ucchwas T. Utsha, and Bashir I. Morshed, Department of Computer Science, Texas Tech University, Lubbock, TX, USA nmitra@ttu.edu, uutsha@ttu.edu, and bmorshed@ttu.edu

Abstract—Electromyography (EMG) signals are very useful for the development of active prosthetic devices and for detecting various muscle abnormalities now-a-days. Many modern technologies are being employed for this purpose, utilizing EMG data to evaluate muscle activity. The existing research on EMG-based movement classification faces the challenges of inaccurate classification, insufficient generalization ability, and weak robustness. To address these problems, this paper proposes a novel EMG signal acquisition system using an Inkjet-printed (IJP) electrode array. IJP EMG electrodes were fabricated on flexible polyimide substrates using silver nanoparticle inks for the conductive layer and provided the flexibility of the shape and size of electrodes. In this work, a classification method with different machine learning (ML) models was performed on the datasets collected from our designed EMG circuit system. We have extracted 145 features from the dataset to properly train and test our ML models. The Random Forest (RF) model yielded a maximum accuracy of 98% for the suggested system. To validate the result, we classified the datasets by using the K-nearest Neighbor Algorithm (90%), Decision Tree (94%), and Artificial Neural Network (97%) and compared the results with the RF model. This proposed method is highly accurate for actuating prosthetics, or it has the ability to maximize medical resources and serve as a clinical auxiliary diagnostic tool.

Keywords: EMG signals, EMG sensors, Feature extraction, Finger movements, Inkjet-printed electrode, Machine learning model

I. Introduction

Electromyography (EMG) research is gaining great impetus nowadays. Much of its credit can be given to the fact that EMG represents the activity of muscles [1]. Collecting surface EMG (sEMG) signals emanating from the human body using electrodes has become a routine procedure both in rehabilitation engineering and medical research. Surface EMG (sEMG) records vital information which is from the muscle action that is responsible for the contraction and extraction of skeletal muscles [2]. The clinically used wet gel electrode where a gel of Ag/AgCl is normally used for getting better skinelectrode coupling in collecting sEMG data is considered the standard electrode. However, because of its disposable nature and irritation to the skin, this electrode is not appropriate for long-term signal monitoring. Also, the gel dries out over time, which degrades the signal quality [3]. Inkjet-printed (IJP) electrodes offer a low-cost and promising solution for efficient sEMG signal analysis. In contrast to gel electrodes, a dry

electrode's efficacy often improves with time as more moisture permeates the skin-electrode contact, increasing coupling. They are designed to be thin, flexible, and conformable to the body, ensuring a more comfortable experience for users, even during prolonged wear. To achieve reliable classification of the sEMG signals for different finger movements, three consecutive phases make up the implementation procedure: data pre-processing, feature extraction, and classification [4]. However, real-world variables like electrode displacement and muscle fatigue can contaminate EMG signals; even little adjustments can have a significant impact on classification outcomes.

To achieve high classification performance and to overcome the limitations of the existing techniques, we proposed a novel approach to develop a affordable EMG signal acquisition system that gathers finger activity using an IJP dry flexible electrode array. The goal of the research is to determine if using EMG data obtained with our newly built IJP electrode array—which can differentiate between different finger movements is advantageous. We used machine-learning models to classify various movements and estimate the user's state. The accuracy results were compared to find the best model. Through the analysis of the EMG signals obtained from our suggested system, we can create a process that will help understand the patient's state and any muscle abnormalities.

II. EXPERIMENTAL SETUP

A. Electrode Fabrication

To capture real-time EMG data, we created dry EMG electrodes on flexible polyimide films using Inkjet Printing (IJP). We have designed this new electrode layout for collecting EMG because we have seen that if we placed positive and negative electrodes in the liner line with every finger then we can get the best EMG signal for the fingers. So to collect EMG for 5 fingers we have designed 5 positive points in upper line and 5 negative points in lower line so that when we placed the whole electrode on the back of the palm, they stayed in the liner line with the fingers. The fabrication process involved the utilization of a PC-controlled Dimatix Materials Printer (DMP-2850, FujiFilm Inc., USA) equipped with a MEMS-based printer cartridge containing 12 linearly arranged printing nozzles with 338.67 μ m gaps, with the cartridge head angle

set at 2.5°. This results in a 15 μ m drop spacing at a printing resolution of 1693 dpi.

The polyimide film substrate served as the foundation for our fabrication. the film was cleaned properly with isopropyl alcohol to remove all the dust. Subsequently, silver nanoparticle (AgNP) ink, Metalon® JS-A191 (Novacentrix Inc., TX, USA) was injected into the substrate using the DMP printer to create the conductive layer. The Silver A191 ink is composed of 40% silver nanoparticles by weight, featuring a silver concentration ranging from 25% to 50%. It includes 10-15% ethylene glycol and 0.2 - 1% polyethylene glycol 4-(tertoctylphenyl) ether as part of its formulation. At 25°C, the ink exhibits a viscosity ranging from 8 to 12 cP, and its surface tension falls between 28 to 32 dyne/cm. The average particle size (Z-avg) of JS-A191 ink is between 30 and 50 nm which has a specific gravity of 1.6. In the IJP process, the ink is ejected drop by drop from the cartridge nozzle in a left-toright printing direction on the polyimide substrate.

After printing, we cured it at 180° temperature for 20 minutes. The choice of Metalon® JS-A191 silver nanoparticle (AgNP) ink was driven by its high conductive properties and compatibility with polyimide. We used an anchoring cavity construction technique to improve substrate adherence and boost the reusability of large-area traces, such as pads. The printed layers contain deliberate gaps created by these holes. These spaces are meant to relieve the thin-film remnants of stress. They successfully lessen the possibility of surface stress mismatch between the printed thin-film and substrate, which lowers the risk of adhesion-related problems like delamination and attachment to the body. This method guarantees that the traces will remain functional and intact even after numerous uses. The electrode layout is shown in Fig. 1

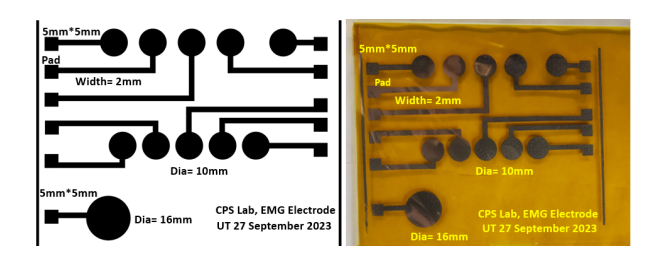


Fig. 1. (Left) EMG electrode array layout design. (Right) An IJP fabricated EMG electrode array.

B. System Overview

The system consists of an EMG signal collection technique which is based on an AD8232 (Analog Devices, Wilmington, MA) and Arduino Uno with an ATmega 328 microcontroller connected with the IJP electrode. To record the EMG signals in the mV range, an IJP electrode array is placed on the back of the palm with the use of transparent silicone tape. In Fig. 2 the overall methods of the EMG signal acquisition process are shown.

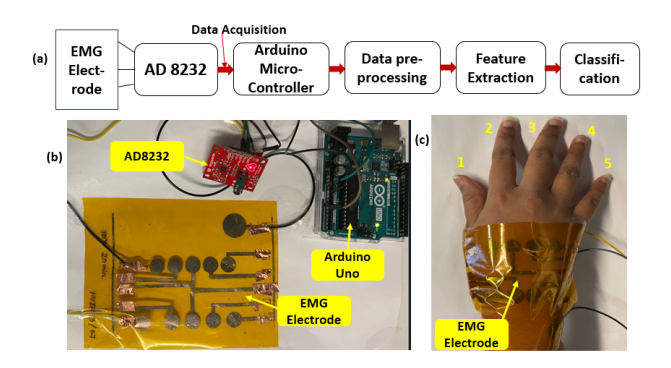


Fig. 2. a) Basic steps of EMG signal classification b) Circuit setup for EMG signal acquisition c) A practical setup of a user wearing the electrode array and numbering of fingers

III. METHODOLOGY

A. Data Acquisition

5 participants' (Age range: 25-35 years old) EMG data were collected at a 100 Hz sampling rate for various movements for the duration of 15 minutes each. We adhered to a methodology consisting of several steps in order to ensure a similar data collection for each participant for every finger one by one. The steps are as follows:

- 1) After positioning the EMG electrode array on the back of the hand, keep the hand in a still and relaxed position for 20 sec.
- 2) After that, rotate one finger for 20 sec in both clockwise and counterclockwise directions, then hold the hand stationary for 10 sec.
- After that, move the finger for 20 sec in each direction—up, down, and left, right.
- At last, keep the hand in a still and relaxed position for 20 sec and we saved the EMG data in CSV format.

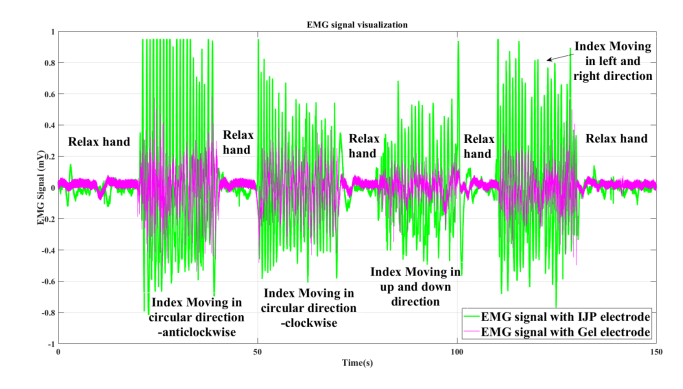


Fig. 3. Data visualization of EMG signal using IJP electrode and gel electrode

B. Data Visualization

A practical setup of a user wearing the electrode is shown in Fig. 2 (c) for reference. We have also collected the EMG signal with commercial gel electrodes (Red Dot Electrodes 2560, 3M, Maplewood, MN) and plotted them with the fabricated IJP electrode-acquired EMG signal to compare both signals for

all the participants. The plot for participant 1 is shown in Fig. 3 for reference. The thumb finger is designated as finger 1, the remaining are as fingers 2, 3, 4 and 5 as depicted in Fig. 2(c). We used the following formula to determine the signal-to-noise ratio (SNR) [6] of both of the EMG signals we had collected:

$$SNR = 10 \log (S/N)$$

where S represents the raw signal power and N shows

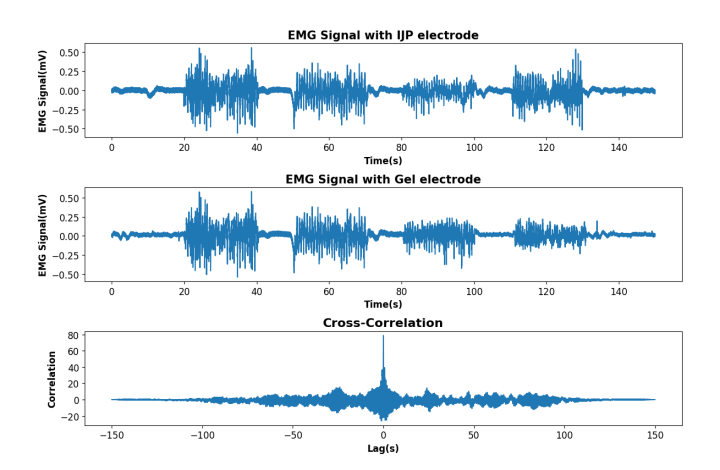


Fig. 4. Cross-correlation between two EMG signals from IJP electrode and gel electrode

the noise power. The SNR for gel and IJP electrode were 18.97 dB and 18.94 dB respectively for user 1. We also calculated the SNR for other users to compare the results. To see the correlation between two EMG signals, we calculated the Pearson correlation coefficient which is 0.7132364631, suggesting a strong positive linear relationship. To visualize the cross-correlation between the signals, we have plotted the signals in Fig. 4.

C. Data Processing

Feature extraction from unprocessed data is an essential stage in data processing [5]. We extracted several features and ranked the top 10 features in order to obtain an accurate detection and apply the machine learning models. Those features are outlined in Table I.

 ${\bf TABLE~I} \\ {\bf TOP~10~Features~Extracted~for~Machine~Learning~Algorithm} \\$

Features		
0_MFCC 8	0_Peak to peak distance	0_FFT mean coeffi_2
0_Spectral centroid	0_Spectral decrease	0_LPCC 10
0_Spectral kurtosis	0_Spectral skewness	0_Spectral slope
0_Spectral spread		

We have used 4 machine learning models to assess the dataset we have gathered. They are the Artificial Neural Network (ANN), Decision Tree (DT), Random Forest (RF), and K-nearest Neighbor (KNN). Because model training is the process by which a machine learning model learns from

the supplied data to produce accurate classifications on fresh, unseen data, it is essential for a classifying task [7].

We divided our dataset into two categories for training.In the first group, the dataset was divided into a training set (80%) and a testing set (20%). In the second method, the whole dataset has been divided into three groups: testing, validation, and training sets, which make up 70%, 15%, and 15% of the total. This enables us to validate the model's performance and assess our models on an alternative testing set. We also applied a 10-fold CV to all models to lessen the variance in performance. After our dataset was trained using the best parameter variation configuration for each of our three dataset distributions, accuracy and performance measures were computed.

IV. RESULTS

The acquired datasets' various finger movement variations are categorized into classes, which are shown in Table II. We have gathered datasets containing all of these classes for each finger, for a total of 25 classes in the class variation. Some of the examples are "Relax_1", "Cir-Anti_1" for thumb finger, "Cir-clock_2", "Up/Down_2", "Left/Right_2" for Index finger. We have computed various statistical metrics to compare the results of all ML models. In addition to training and testing accuracy, we also determined the error metrics as Root Mean Squared Error (RMSE), Mean Absolute Error (MAE), and Rsquared [8] to evaluate the best performing ML method which are listed in Table III.A confusion matrix is a particular type of matrix that is used to show how well a machine learning algorithm performs. In this matrix, each row denotes the actual category and each column the predicted value. The confusion matrix for a 10-fold CV is represented in Fig. 5.

TABLE II DIFFERENT CLASS LIST

Position	Target class
Hand in still and relax position	Relax Hand
Finger moving in Circular direction - Anticlockwise	Cir-Anti
Finger moving in a Circular direction - clockwise	Cir-Clock
Finger moving in up and down direction	Up/Down
Finger moving in left and right direction	Left/Right

V. DISCUSSION

Reusable IJP electrodes excelled gel electrodes which offer superior performance without causing skin irritation. They proved comfortable for users and effectively captured EMG signals during finger movements. From the correlation graph, we can say that the two EMG signals are strongly correlated, implying that the muscle activities recorded by these signals are synchronized to a significant extent. From our calculated results for every test subject, we can state that the RF model performs better than all ML models in terms of categorizing distinct finger movements. In every one of our tests, the RF model has continuously performed better, with an accuracy rate as high as 98%. Large and complicated datasets with millions of observations and thousands of characteristics can

TABLE III
PRESENTATION OF ALL THE MODELS' PERFORMANCE INDICATORS FOR VARIOUS DATASET SPLITS FOR DIFFERENT FINGER MOVEMENTS

	Data	aset with	n 80/20	split	Datas	et with	70/15/15	5 split	10-fold cross validation					
	KNN	RF	DT	ANN	KNN	RF	DT	ANN	KNN	RF	DT	ANN		
Training set accuracy (%) ↑	86	95	94	95	89	97	94	97	90	98	94	98		
Testing set accuracy (%) ↑	85	94	93	94	89	97	94	96	90	98	94	97		
RMSE ↓	0.94	0.33	0.41	0.66	0.84	0.36	0.45	0.53	0.79	0.2	0.41	0.44		
MAE ↓	0.31	0.04	0.08	0.14	0.24	0.05	0.1	0.09	0.22	0.02	0.08	0.05		
R-squared ↑	0.84	0.96	0.95	0.92	0.87	0.98	0.96	0.95	0.89	0.99	0.97	0.97		

_																									
Relax_1	1270	0	0	o	0	0	o	0	0	0	0	0	0	0	0	0	0	0	0	0	0	0	0	0	0
Cir-Anti_1	0	384	0	0	0	0	0	0	9	0	0	0	0	0	0	0	0	0	0	0	0	0	0	0	0
Cir-clock_1	o	o	458	7	0	o	o	o	o	0	o	o	o	o	o	0	o	o	0	o	o	o	0	0	o
Up/Down_1	0	o	o	424	0	o	0	o	o	o	0	o	o	0	o	o	0	o	4	o	o	0	o	o	o
Left/Right_1	o	o	o	o	391	o	o	o	1	o	o	o	o	o	9	o	o	o	o	o	o	o	0	o	o
Relax_2	0	o	0	o	0	461	7	o	7	o	o	o	0	o	o	0	o	o	0	o	0	0	0	o	o
Cir-Anti_2	o	o	0	o	0	0	335	0	53	0	o	o	0	o	o	0	o	o	0	o	0	o	0	o	o
Cir-clock_2	0	0	0	0	0	o	5	348	46	0	o	0	0	0	2	0	0	o	0	o	0	o	0	0	o
Up/Down_2	o	0	o	o	0	o	o	0	404	0	o	o	0	o	o	0	o	o	0	o	o	o	0	o	o
Left/Right_2	o	o	o	o	О	o	o	o	О	1319	o	o	o	o	o	o	o	o	o	o	o	o	o	o	o
Relax_3	o	o	o	o	o	o	o	o	o	0	L329	o	o	o	o	o	o	o	o	o	o	o	o	o	o
Cir-Anti_3	o	o	o	o	o	o	2	o	8	o	o	428	o	o	o	o	o	o	o	o	o	o	o	o	o
Cir-clock_3	o	o	o	o	o	o	4	o	45	o	o	o	358	o	o	o	o	o	o	2	o	o	o	o	o
≪ Up/Down_3 -	o	o	o	o	o	o	o	o	o	o	o	o	o	399	o	o	o	o	o	o	o	o	o	o	o
Left/Right_3	o	o	o	o	o	o	o	o	31	o	o	o	o	o	426	0	o	o	o	o	o	o	o	o	o
Relax_4	o	o	o	o	o	o	o	o	o	o	o	o	0	o	О	1329	o	o	7	o	o	o	0	o	o
Cir-Anti_4	0	o	o	o	o	o	o	o	27	o	o	o	o	o	o	o	417	o	o	o	o	o	0	o	o
Cir-clock_4	o	o	o	o	o	o	6	o	25	o	o	o	o	o	o	o	О	405	o	o	o	o	o	o	5
Up/Down_4	o	О	o	o	o	o	o	o	o	o	o	o	o	o	o	o	o	О	388	o	o	o	o	o	o
Left/Right_4	o	o	o	o	o	o	o	o	o	o	o	o	o	o	o	o	o	o	0	400	o	o	0	o	o
Relax_5	o	o	o	o	o	o	o	o	o	o	o	o	0	o	o	0	o	o	o	0	1249	o	0	o	o
Cir-Anti_5	o	o	o	o	o	o	o	o	16	o	o	o	0	o	o	0	o	o	0	o	0	469	0	o	o
Cir-clock_5	o	o	o	o	o	o	o	o	2	o	o	o	o	o	o	o	o	o	o	o	o	o	460	o	o
Up/Down_5	o	o	o	o	o	o	o	o	8	o	o	o	o	o	o	o	o	o	o	o	o	o	o	421	o
Left/Right_5	o	o	o	o	o	o	o	o	17	o	o	o	o	o	o	o	o	o	o	o	3	o	o	o	458
	×_1.	ţŢ.	X.	<u>_</u>	Ę	×.2	ti_2.	<u>,</u>	n_2.	ıt 2	Relax_3	<u>ti</u> .3	κ,	n_3.	<u>t</u> 3	× 4	ti_4	4	n_4	t_4.	× 5	ti_5.	اج	n_5.	<u>1</u> 5
	Relax_1	Cir-Anti_1	Cir-clock_1	Up/Down_1	Left/Right_1	Relax_2	Cir-Anti_2	Cir-clock_2	Up/Down_2	Left/Right_2	Rela	Cir-Anti_3	Cir-clock_3	Up/Down_3	Left/Right_3	Relax_4	Cir-Anti_4	Cir-clock_4	Up/Down_4	Left/Right_4	Relax_5	Cir-Anti_5	Cir-clock_5	Up/Down_5	Left/Right_5
		U	ō	ď	Left		U	ö	ď	Left			ਂਹੋਂ edicte		Left		U	ō	g	Left		U	ō	ď	Left
													-												

Fig. 5. Visualization of true (actual) class and predicted class for RF model with 10-fold Cross Validation split

be handled by RFs, which are also very scalable. On the other hand, the KNN is often particularly tricky for expansive datasets, and the performance tends to degrade as the dimensionality of the feature increases.

VI. CONCLUSION

An approach to design an EMG signal acquisition system to easily collect the EMG signals from the users' fingers using an IJP EMG electrode array and to classify all 5 finger movements are presented in this paper. We collected EMG data from our IJP electrode simultaneously and compared the data with gel electrodes sold in markets. This study also emphasized the algorithms used for processing, and classifying EMG signals. The outcomes showed that the random forest (RF) model performed better than the other models. Thus, we can use the new fabricated flexible IJP electrodes in

various new EMG wearables and it can also used to enhance the performance of models for disease detection or actuating prosthetics.

ACKNOWLEDGMENT

This material is based upon work supported by the National Science Foundation under Grant No. 2105766.

REFERENCES

- 'Design of a Flexible High-Density Surface Electromyography Sensor', Jirou Feng, Handdeut Chang, Hwayeong Jeong and Jung Kim, 978-1-7281-1990-8/20/IEEE
- [2] Circuit Design and Analysis of an Electromyography (EMG) Signal Acquisition System, Md Zahirul Alam Chowdhury, Divya Pradip Roy, 978-1-7281-9877-4/20/
- [3] M. M. R. Momota, B. I. Morshed, T. Ferdous and T. Fujiwara, "Fabrication and Characterization of Inkjet Printed Flexible Dry ECG Electrodes," in IEEE Sensors Journal, vol. 23, no. 7, pp. 7917-7928, 1 April1, 2023, doi: 10.1109/JSEN.2023.3250103.

- [4] Analysis and Simple Circuit Design of Double Differential EMG Active Electrode', Federico Nicolás Guerrero, Enrique Mario Spinelli, and Marcelo Alejandro Haberman, IEEE Transactions On Biomedical Circuits and Systems, Vol., 10, NO. 3, June 2016
- [5] S. M. Pincus, "Approximate entropy as a measure of system complexity," Proc. Natl. Acad. Sci. U. S. A., Vol. 88, no. 6, pp. 2297–2301, 1991.
 [6] 'Different techniques for EMG signal processing', Vibromechanika.
- [6] 'Different techniques for EMG signal processing', Vibromechanika. Journal Of Vibroengineering. 2008 December, Vol 10, Issue 4, ISSN 1392-8716 J. Pauk,
- [7] S. Benatti, F. Montagna, V. Kartsch, A. Rahimi, D. Rossi, L. Benini, Online learning and classification of EMG-based gestures on a parallel ultra-low power platform using hyperdimensional computing, IEEE Transactions on Biomedical Circuits and Systems 13(3)(2019)516–528.
- Transactions on Biomedical Circuits and Systems 13(3)(2019)516–528.
 [8] Willmott, Cort J., and Kenji Matsuura. "Advantages of the Mean Absolute Error (MAE) over the Root Mean Square Error (RMSE) in Assessing Average Model Performance." Climate Research, vol. 30, no. 1, 2005, pp. 79–82, JSTOR, 2024